



**DYNAMIC RESERVOIR
SIMULATION MODEL
DYRESM v4**

v4.0 Science Manual

Imerito, A.

Centre for Water Research
University of Western Australia.
February 20, 2007

Contents

List of Figures	v
List of Tables	vii
1 DYRESM Overview	1
1.1 DYRESM Overview	1
1.1.1 The DYRESM numerical model	1
1.1.2 The program	1
2 Introduction	3
2.1 Introduction	3
2.1.1 One Dimensional Assumption	3
3 The Layer Structure	7
3.1 The Layer Structure	7
3.1.1 Introduction	7
3.1.2 Volume, Area and Thickness Relationship	7
3.1.3 Thickness Limits of the Layers	8
3.1.4 The Equation for Density in Each Layer	9
3.1.5 Checking Layer Stability	10
3.1.6 Conservation Laws	10
4 Surface Heat, Mass and Momentum Exchange	11
4.1 Surface Heat, Mass and Momentum Exchange	11
4.1.1 Introduction	11
4.1.2 Surface energy fluxes	12
4.1.3 Surface mass fluxes	18
4.1.4 Surface momentum fluxes	18
4.1.5 Surface layers re-gridding	20
4.1.6 Atmospheric stability and surface exchange	20
5 Surface mixed layer algorithm	21
5.1 The Surface Mixing Model	21
5.1.1 Mechanisms	21
5.1.2 Energetics	21
5.1.3 Method	22

5.1.4	Epilimnion and hypolimnion information	23
5.1.5	Bottom stresses	23
6	Inflow Dynamics	25
6.1	Inflow Dynamics	25
6.1.1	Surface Inflow	25
6.1.2	Subsurface inflow	28
7	Outflow Dynamics	31
7.1	Outflow Dynamics	31
7.1.1	Withdrawal	31
7.1.2	Overflow	31
7.1.3	Data Output	31
8	Deep Mixing	33
8.1	Deep Mixing	33
8.1.1	Introduction	33
8.1.2	Solution Method	33
9	Artificial Destratification	37
9.1	Artificial Destratification	37
9.1.1	Bubble Plume Diffusers	37
9.1.2	Surface mechanical mixers with draft tubes	39
A	Bibliography	41

List of Figures

2.1	Definition sketch of variables used in derivation of the Lake number.	4
3.1	Definition of the height and thickness of a layer. DYRESM defines the height of a layer from the bottom of the reservoir.	7
4.1	Surface energy flux exchanges.	12
4.2	Short wave radiation distribution using daily average input data.	14
6.1	Possible river inflow patterns.	26
6.2	Schematic diagram of downflow aliquot.	27

List of Tables

3.1	Coefficients for equation 3.8	9
3.2	Coefficients for equation 3.9	9
4.1	Meteorological Data	11

DYRESM Overview

1.1 DYRESM Overview

1.1.1 The DYRESM numerical model

DYRESM (DYnamic REServoir Simulation Model) is a one-dimensional hydrodynamics model for predicting the vertical distribution of temperature, salinity and density in lakes and reservoirs satisfying the one-dimensional approximation.

The one-dimensional approximation is valid when the forces acting to destabilize a water body (wind stress, surface cooling or plunging inflows) do not act over prolonged periods of time. The dynamics of many lakes and reservoirs, viewed over time scales longer than those of extreme events such as storms and floods, are well described using this approximation. DYRESM provides quantifiably verifiable predictions of the thermal characteristics in such systems over time scales ranging from several weeks to tens of years. The model thus provides a means of predicting seasonal and inter-annual variability of lakes and reservoirs as well as sensitivity testing to long-term changes in environmental factors or watershed properties. DYRESM can be run either in isolation for purely hydrodynamic studies or coupled to CAEDYM (Computational Aquatic Ecosystem DYNAMics Model) for investigations involving biological and/or chemical processes. The computational demands of DYRESM are quite modest and multi-year simulations can be carried out on PC platforms under Windows or Linux.

The DYRESM computer model parameterizes the important physical processes leading to temporal changes in the temperature, salinity and density distributions in lakes and reservoirs. The model relies on parameterizations derived from detailed process studies (both from the field and in the laboratory) and thus draws on the internationally recognized strengths of the Centre for Water Research in analytical, laboratory and field measurement of density-stratified flows. The resulting model is unique in that reliable predictions are obtained without calibration of model parameters.

1.1.2 The program

<i>Implementation Language:</i>	Fortran 95
<i>Development Platform:</i>	Linux
<i>Target Platforms:</i>	The source code is written using only standard Fortran 95 so the source code is 'copy-portable'
<i>Program Architecture:</i>	DYRESM has a layered program architecture. The science routines are abstracted from the I/O and to a lesser extent – from the data structure of the model.

The set of science procedures and data structures were designed and built as an object-oriented (OO) core to DYRESM. This provides good encapsulation for the code, readily allows extension and matches closely the

abstract conceptualization of the DYRESM model. (Even though Fortran 95 is an object-**based** (rather than an object-oriented) language an OO design can still be implemented – albeit with more effort.)

Introduction

2.1 Introduction

DYRESM (DYnamic REservoir Simulation Model) is a one-dimensional hydrodynamics model for lakes and reservoirs, and is used to predict the variation of water temperature and salinity with depth and time. The hydrodynamic component is a process based model, as opposed to empirically based, and does not require calibration. The model forms the one-dimensional hydrodynamics driver to the CAEDYM water quality model.

The model DYRESM is based on an assumption of one dimensionality; that is, the variations in the vertical play a more important role than those in the horizontal direction. This gives rise to the layer construction, in which the reservoir is represented as a series of horizontal layers. There is no lateral or longitudinal variation in the layers, and the vertical profile in any property is obtained from the property values from each layer.

In DYRESM these layers are of different thicknesses; as inflows and outflows enter or leave the reservoir, the affected layers expand or contract and those above move up or down to accommodate the volume change. The vertical movement of layers is accompanied by a thickness change as the layer surface areas change with vertical position in accord with the reservoir bathymetry. Mixing is modelled by amalgamation of adjacent layers, and the layer thicknesses are dynamically set internally by the model to ensure that for each process, an adequate resolution is obtained.

2.1.1 One Dimensional Assumption

The one-dimensional assumption is based on observations that the density stratification usually found in lakes inhibits vertical motions while horizontal variations in density are quickly relaxed by horizontal advection and convection. Horizontal exchanges generated by weak temperature gradients are communicated over several kilometres on time scales of less than a day, suggesting that the one-dimensional model is suitable for simulations over daily time scales.

The validity of the one-dimensional assumption is tested against the Lake number LN (Imberger and Patterson, 1990). The Lake number is defined in terms of the stability of the stratification and the disturbing influence of the wind. Consider a general lake with an arbitrary stratification $r(z)$ being acted upon by a general wind field with a surface friction velocity u_* . Figure 2.1 presents a definition sketch of variables used in derivation of the Lake number.

As this wind stress is imposed on the surface layer, there will be a net force acting to overturn the density structure of the water column. Taking moments about the center of volume located at z_g for the whole lake body, we obtain for equilibrium

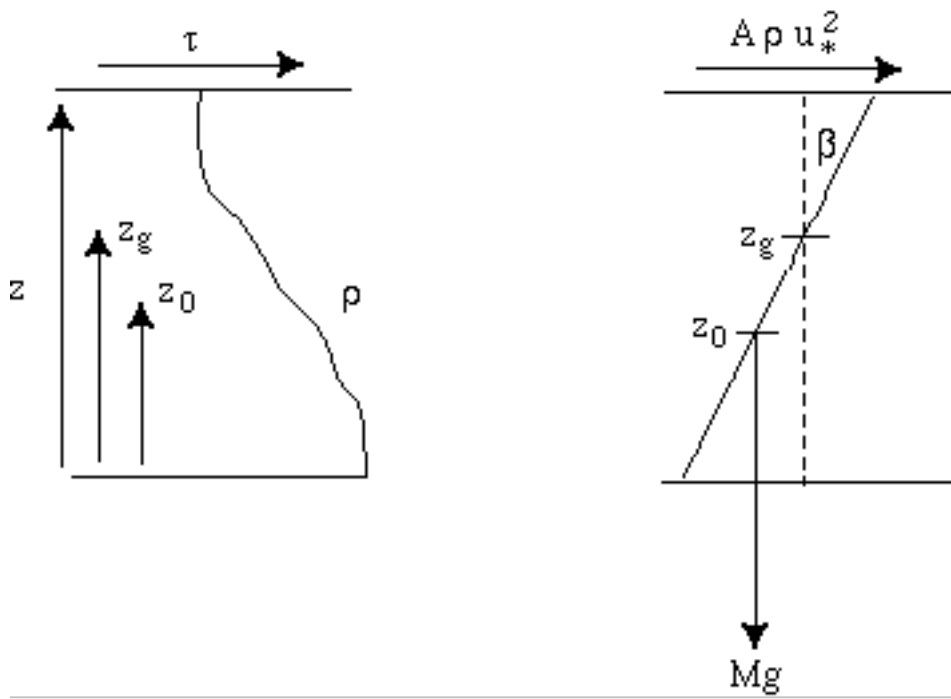


Figure 2.1 Definition sketch of variables used in derivation of the Lake number.

$$(z_H - z_g) \int_{A(z_H)} \rho_o u_*^2 dA = (z_g - z_o) Mg\beta \quad (2.1)$$

where z_H is the height of the water column, z_o is the center of gravity of the water mass with a density stratification $r(z)$ at height z above the lake bottom, M is the total mass of water, and β is the angle subtended to the vertical by the line segment connecting the center of mass to the center of volume (β is assumed to be small; i.e. $\beta \approx \tan\beta$). This leads to the Lake number

$$L_N = \frac{(z_g - z_o) Mg\beta}{\int_{A(z_H)} \rho_o u_*^2 dA (z - z_g)} \quad (2.2)$$

where z_o is defined by

$$z_o = \frac{\int_0^{z_H} \rho(z) z A(z) dz}{\int_0^{z_H} \rho(z) A(z) dz} \quad (2.3)$$

The maximum deflection occurs when the thermocline reaches the surface, so that

$$\beta = \frac{z - z_T}{\sqrt{A(z)}} \quad (2.4)$$

where z_T is the height to the center of the metalimnion. This gives

$$L_N = \frac{z_g - z_o Mg \left(1 - \frac{z_T}{z}\right)}{\sqrt{A} \left(1 - \frac{z_g}{z}\right) \int_{A(z_H)} \rho_o u_*^2 dA} \quad (2.5)$$

Assuming that the wind stress is constant over the surface, then L_N reduces to

$$L_N = \frac{z_g - z_o Mg \left(1 - \frac{z_T}{z}\right)}{A^{3/2} \left(1 - \frac{z_g}{z}\right) \rho_o u_*^2} \quad (2.6)$$

If $L_N \gg 1$, then the restoring force is greater than the disturbing force, and the deflection of z_o is small. This means that the density structure will be approximately horizontal and the one dimensional assumption is valid. Physically this means that the lake stratification will be severe and dominate the forces introduced by the surface wind stress. Under these circumstances stratification is expected to be horizontal with little or no seiching and little turbulent mixing in the metalimnion or the hypolimnion. The criterion for one dimensionality is then $L_N \gg 1$.

A similar criterion may be developed for disturbances due to inflows, where the disturbing force is the action of the inflows. This yields

$$L_{N_i} = \frac{z_g - z_o Mg \left(1 - \frac{z_T}{z}\right)}{A^{1/2} u Q \left(\frac{z_g - z_i}{z}\right)} \quad (2.7)$$

where z_i is the depth of the inflow and u is the inflow speed. For one dimensionality, $L_{N_i} \gg 1$. Physically this means the stratification will quickly dampen horizontal disturbances due to intruding inflows. The stratification will force the density structure to remain approximately horizontal and all horizontal disturbances will be quickly relaxed.

A final criteria to check is for the effects of the earth's rotation (Patterson *et al* 1984). This is defined by the ratio

$$R = \frac{R_I}{B} \quad (2.8)$$

where R_I is the internal Rossby radius of deformation and B is the maximum width of the lake. The internal Rossby radius is defined as

$$R_i = \frac{g' h}{f} \quad (2.9)$$

where g' is the effective reduced gravity over the surface layer depth h , and f is the Coriolis parameter. For $R > 1$, the assumption of one-dimensionality holds.

Note that DYRESM does not perform these calculations, and it is up to the user to determine whether the one-dimensional assumption is valid for the particular application.

The Layer Structure

3.1 The Layer Structure

3.1.1 Introduction

DYRESM is based on a Lagrangian layer scheme (i.e., the layers are adjusted to stay within user-defined limits; a fixed grid approach would be a Eulerian scheme) in which the lake is modelled by a series of horizontal layers of uniform property but variable thickness. The layer positions change as inflow, outflow, evaporation and rainfall affect the stored volume, and layer thicknesses change as the layers are moved vertically to accommodate volume changes.

The additional advantage of this layer scheme is that it lends itself to the vertical structure of the lake. For example, the mixed layer in which the properties of the species can be considered mostly constant over depth can be modelled as a single layer in this layer scheme. On the other hand layers can be very narrow over areas of large vertical gradients in properties, for example, the thermocline.

3.1.2 Volume, Area and Thickness Relationship

This relationship calculates the layer volumes and surface areas corresponding to given layer thicknesses or conversely, layer thicknesses and surface areas corresponding to given volumes. The relationship is used following any operation which affects either volumes or thicknesses. Note that layers are counted from bottom to top (see Figure 3.1).

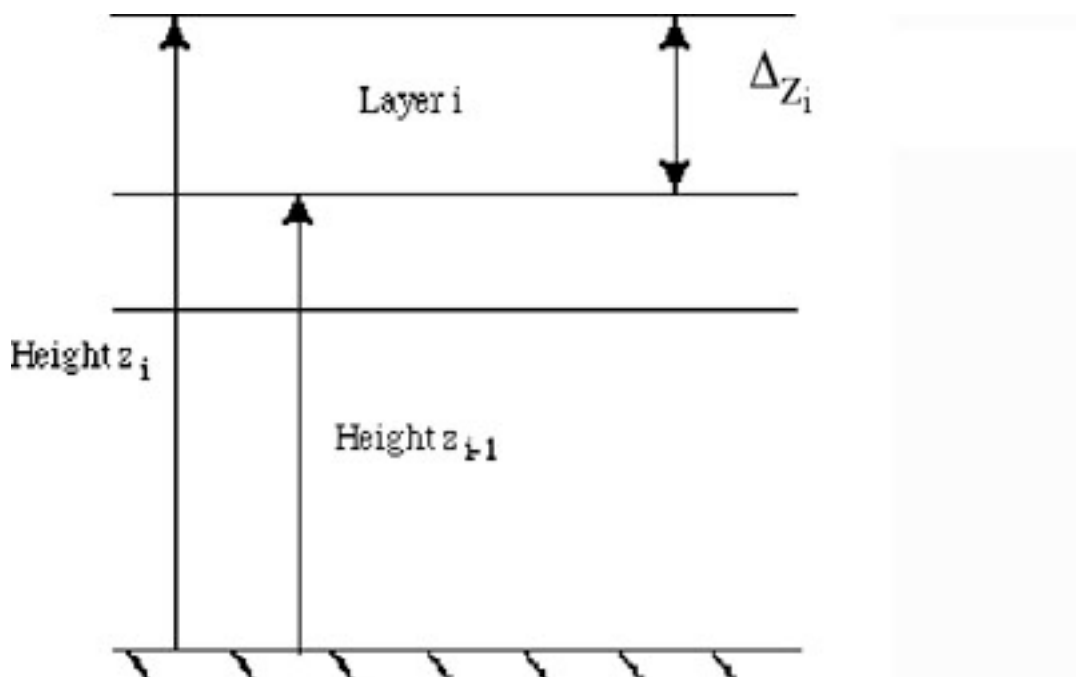


Figure 3.1 Definition of the height and thickness of a layer. DYRESM defines the height of a layer from the bottom of the reservoir.

The calculation is an interpolation on the given height-volume-area data for the reservoir. Thus, consider one of these Lagrangian layers. At time t_{i-1} the layer has a certain thickness, area and volume. At time t_i a process has changed either the thickness or volume of the layer. As a result it will now have a new thickness, area and volume.

The layer structure is based on layers having curved sides. Volumes are calculated cumulatively from the base upwards, with

$$V(z) = V_{k-1} \left(\frac{z}{z_{k-1}} \right)^{a_k}; \quad 0 < z_{k-1} < z \leq z_k \quad \forall k \in \{2, 3, \dots, N_S\} \quad (3.1)$$

and

$$A(z) = A_{k-1} \left(\frac{z}{z_{k-1}} \right)^{b_k}; \quad 0 < z_{k-1} < z \leq z_k \quad \forall k \in \{2, 3, \dots, N_S\} \quad (3.2)$$

where

$$a_k = \frac{\log \frac{V_k}{V_{k-1}}}{\log \frac{z_k}{z_{k-1}}} \quad \forall k \in \{2, 3, \dots, N_S\} \quad (3.3)$$

and

$$b_k = \frac{\log \frac{z_k}{z_{k-1}}}{\log \frac{z_k}{z_{k-1}}} \quad \forall k \in \{2, 3, \dots, N_S\} \quad (3.4)$$

For the bottom layer, a conical section is used such that

$$A(z) = A_1 \left(\frac{z}{z_1} \right)^2; \quad 0 \leq z \leq z_1 \quad (3.5)$$

and hence

$$V(z) = V_1 \left(\frac{z}{z_1} \right)^3; \quad 0 \leq z \leq z_1 \quad (3.6)$$

3.1.3 Thickness Limits of the Layers

Limits are set on the individual layer thicknesses and volumes. The upper and lower limits are set to ensure that adequate resolution is achieved and that an excessive number of layers is not used. However, a constraint on the lower limit is that it must be small enough so that numerical diffusion problems do not arise through an excessive number of layer amalgamations. Any layers with volumes in excess of the allowable maximum volume are split in the required portions, creating new layers with identical properties but with volumes reduced. The layers are renumbered and the surface areas determined. Similarly for layers with volume less than the allowable

minimum, they are amalgamated with the neighbouring layer of smallest volume, the layers renumbered and the surface areas determined.

3.1.4 The Equation for Density in Each Layer

Density is a measure of a solution's mass per unit volume. The density of a solution usually decreases as temperature increases and increases as the solute concentration (salinity) increases. At 20 °C freshwater has a density 998 kg/m³ while seawater has a density of approximately 1030 kg/m³.

The density of the water (in kg/m³) in a layer given its temperature (°C), salinity (psu), pressure (bars: 1bar = 105 Pa) is given by the UNESCO (1981) equation of state for the density of salt water.

$$\rho(T, S, P) = \frac{\rho(T, S, 0)}{\left(1 - \frac{P}{K(T, S, P)}\right)} \quad (3.7)$$

where

$$\rho(T, S, 0) = A + BS + CS^{3/2} + DS^2 \quad (3.8)$$

where A , B , C and D are polynomial functions of temperature.

Table 3.1: Coefficients for equation 3.8

	A	B	C	D
T^0	+999.8425	$+8.245 \times 10^{-1}$	-5.725×10^{-3}	$+4.831 \times 10^{-4}$
T^1	$+6.794 \times 10^{-2}$	-4.089×10^{-3}	$+1.022 \times 10^{-4}$	
T^2	-9.095×10^{-3}	$+7.643 \times 10^{-5}$	-1.654×10^{-6}	
T^3	$+1.002 \times 10^{-4}$	-8.246×10^{-7}		
T^4	-1.120×10^{-6}	$+5.387 \times 10^{-9}$		
T^5	$+6.536 \times 10^{-9}$			

and

$$K(T, S, P) = E + FP + GP^2 \quad (3.9)$$

where E , F and G are also polynomial functions of temperature.

Table 3.2: Coefficients for equation 3.9

	E	F	G
T^0	$19652.21 + 54.675S + 7.944 \times 10^{-2}S^{3/2}$	$3.240 + 2.284 \times 10^{-3}S + 1.91075 \times 10^{-4}S^{3/2}$	$8.510 \times 10^{-5} - 9.935 \times 10^{-7}S$
T^1	$148.421 - 0.604S + 1.648 \times 10^{-2}S^{3/2}$	$1.437 \times 10^{-3} - 1.098 \times 10^{-5}S$	$-6.123 \times 10^{-6} + 2.081 \times 10^{-8}S$
T^2	$-2.327 + 1.1 \times 10^{-2}S - 5.301 \times 10^{-4}S^{3/2}$	$1.161 \times 10^{-4} - 1.608 \times 10^{-6}S$	$5.279 \times 10^{-8} + 9.170 \times 10^{-10}S$
T^3	$1.360 \times 10^{-2} - 6.167 \times 10^{-5}S$	-5.779×10^{-7}	
T^4	-5.155×10^{-5}		

3.1.5 Checking Layer Stability

The stability of the layer structure is checked by comparing the density of the layers. This check is done by starting with the surface layer and comparing the density with the layer directly below it. If the density of the overlying layer is more than the density of the layer below it, the layers are combined, the properties of the two layers are conserved according to the equations governing constituent conservation and the new density determined from the new temperature and salinity. The density of this layer is then compared to the next layer below it and the process repeated until the lower most layer is reached. This process ensures that the density profile is always stable.

3.1.6 Conservation Laws

When combining two layers, the conservation laws for temperature, salt, energy and momentum can be generalised as

$$C_t^* = \frac{C_i \Delta M_i + C_{i+1} \Delta M_{i+1}}{\Delta M_i + \Delta M_{i+1}} \quad (3.10)$$

where the subscripts refer to layer indices, and C is the property being conserved (q_i , S_i or U_i). For conservation of temperature, the above assumes the specific heat to be constant.

Surface Heat, Mass and Momentum Exchange

4.1 Surface Heat, Mass and Momentum Exchange

4.1.1 Introduction

The surface heat, mass and momentum exchange comprise the primary driving mechanisms for DYRESM. It is these surface exchanges that input the majority of the energy for heating, mixing and stratifying the lake. The surface exchanges include heating due to short wave radiation penetration into the lake and the fluxes at the surface due to evaporation, sensible heat (i.e. convection of heat from the water surface to the atmosphere), long wave radiation and wind stress (Figure 4.1).

The meteorological data used by DYRESM can be either daily or sub-daily. If daily data is entered, all data except shortwave and wind speed are assumed to be uniformly distributed throughout the day. The shortwave energy distribution throughout the day is computed based on the lake latitude and the time of the year. The wind speed can be either uniformly distributed, or have a simple “wind hump” distribution applied. This is described in detail later in the chapter. If sub-daily data are entered, all data are uniformly distributed within the input timestep. The sub-daily timestep must be greater than (or equal to) 10 minutes (600 seconds), and less than (or equal to) 3 hours (10800 seconds).

Short wave radiation (280nm to 2800nm) is usually measured directly. Long wave radiation (greater than 2800nm) emitted from clouds and atmospheric water vapour can be measured directly or calculated from cloud cover, air temperature and humidity. The reflection coefficient, or albedo, of short wave radiation varies from lake to lake and depends on the angle of the sun, the lake colour and the surface wave state. The data required is as follows (Table 4.1):

Table 4.1: Meteorological Data

Attributes	Type	Units
short wave radiation	timestep average	W m^{-2}
long wave (cloud cover, atmospheric, total)	timestep average	W m^{-2}
vapour pressure of air	timestep average	h Pa
wind speed	timestep average	m s^{-1}
air temperature	timestep average	$^{\circ}\text{C}$
rainfall	timestep total	m

The approach used in DYRESM is to first calculate the surface energy fluxes; the the surface mass fluxes then derive from these energy fluxes.

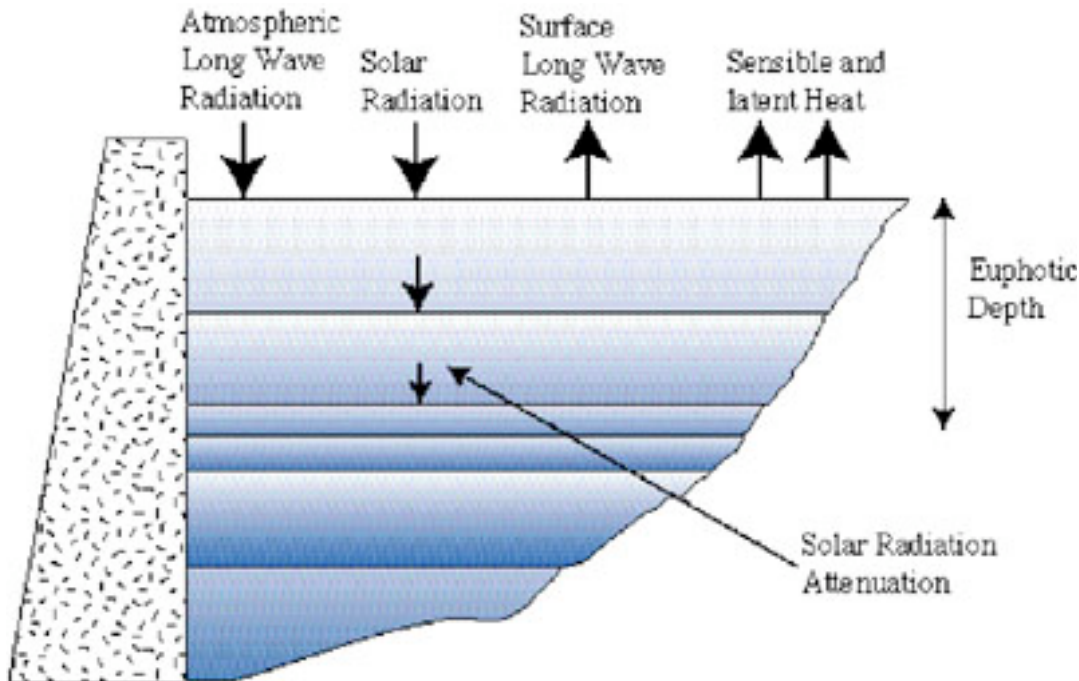


Figure 4.1 Surface energy flux exchanges.

4.1.2 Surface energy fluxes

Determine solar (shortwave) radiation flux

Shortwave radiation can be divided into penetrative and non-penetrative, depending on the wavelength. Radiation shorter than 700 nm (Photosynthetically Active Radiation, or PAR) is considered to be penetrative, meaning that energy is deposited in all layers in the water column, not only the surface layer. This has been found experimentally to be approximately 45% of incoming solar radiation (Gates 1966, Jellison and Melack 1993). DYRESM therefore assumes that 55% of the incoming solar radiation is non-penetrative, with the remaining 45% being distributed throughout the water column. All other fluxes are non-penetrative, and so are absorbed or emitted from the surface layer. Solar (shortwave) radiation is assumed to have a sinusoidal distribution, centred about midday. If a daily timestep is used, the total energy per unit area for a 24 hour period, $Q_{sw(total)}$ is calculated as 45% of the daily average and passed to the thermodynamics routine

$$Q_{sw(total)} = \int_{t_{SR}}^{t_{SS}} A \sin(\omega t - \beta) dt \quad (4.1)$$

The terms in the above equation are described by

$$\omega = \frac{\pi}{N_d \gamma} \quad (4.2)$$

where N_d is the duration of a day (in seconds), t_{SR} is the time of sunrise, t_{SS} is the time of sunset (both in seconds), γ is the day photo fraction (fraction of day with sunlight)

$$\gamma = \frac{t_{SS} - t_{SR}}{N_d}; \quad 0 \leq t_{SR} < t_{SS} < N_d \quad (4.3)$$

and

$$A = \frac{\omega Q_{sw(total)}}{2} \quad (4.4)$$

The day photo fraction is computed based on the lake latitude and the time of the year. The sunset hour angle is first computed as (TVA 1972, eqn2.19; Henderson-Sellers 1986, eqn A5)

$$\cos(h_{ss}) = -\tan \theta \tan \delta \quad (4.5)$$

where θ is the lake latitude, δ is the declination of the sun, computed as (TVA 1972, eqn 2.4)

$$\delta = 23.45 \left(\frac{\pi}{180} \right) \cos \left[\frac{2\pi}{365} (172 - D) \right] \quad (4.6)$$

with D the day of the year. The day photofraction γ is then calculated (TVA 1972, eqn 2.23)

$$\gamma = \frac{h_{ss}}{\pi} \quad (4.7)$$

and t_{SR} and t_{SS} determined by assuming the day is symmetric about midday.

Note that the constraints on t_{SR} and t_{SS} mean that this model is applicable for sub-polar latitudes only. Also note that the solar altitude at sunrise and sunset is assumed to be zero. The term β (radians) is a phase shift to ensure the shortwave radiation curve is symmetrical about midday,

$$\beta = \frac{1}{2} \left(\frac{1}{\gamma} - 1 \right) \pi \quad (4.8)$$

Hence the energy deposited per unit area between the times of t_1 and t_2 ($t_{sr} \leq t_1 < t_2 \leq t_{ss}$) is given by

$$Q_{sw(total)}(t_1, t_2) = A \int_{t_1}^{t_2} \sin(\omega t - \beta) dt \quad (4.9)$$

which results as

$$Q_{sw(total)}(t_1, t_2) = \frac{1}{2} Q_{sw(total)} [\cos(\omega t_1 - \beta) - \cos(\omega t_2 - \beta)] \quad (4.10)$$

For sub-daily meteorological input data, the value of shortwave radiation for a timestep is simply taken from the input data file. Once again, 55% is absorbed in the surface layer, with 45% being distributed according to the Beer-Lambert law.

The next step is to consider the effect of the albedo of the water surface on the penetration of short-wave radiation. We define

$$Q_{sw(total)}(t_1, t_2) = (1 - r_a^{(sw)}) Q_{sw(total)}(t_1, t_2) \quad (4.11)$$

where

$$r_a^{(sw)} = \bar{R}_a^{(sw)} + a^{(sw)} \sin\left(\frac{2\pi d}{D} - \frac{\pi}{2}\right); \quad \text{S}^{\text{th}} \quad \text{Hemisphere} \quad (4.12)$$

$$r_a^{(sw)} = \bar{R}_a^{(sw)}; \quad \text{Equator} \quad (4.13)$$

$$r_a^{(sw)} = \bar{R}_a^{(sw)} + a^{(sw)} \sin\left(\frac{2\pi d}{D} + \frac{\pi}{2}\right); \quad \text{N}^{\text{th}} \quad \text{Hemisphere} \quad (4.14)$$

and

$\bar{R}_a^{(sw)} = 0.08$, $a^{(sw)} = 0.02$, D the standard number of days in a year ($=365$) and d is the day number in the year; $d \in \{1, 2, \dots, D\}$.

Short-wave radiation penetrates according to the Beer-Lambert law, such that

$$Q_x(t_1, t_2) = Q_{sw}(t_1, t_2) e^{-\eta_A x} \quad (4.15)$$

where x is the depth below the water surface (measured down from the surface of the reservoir) and η_A the attenuation coefficient.

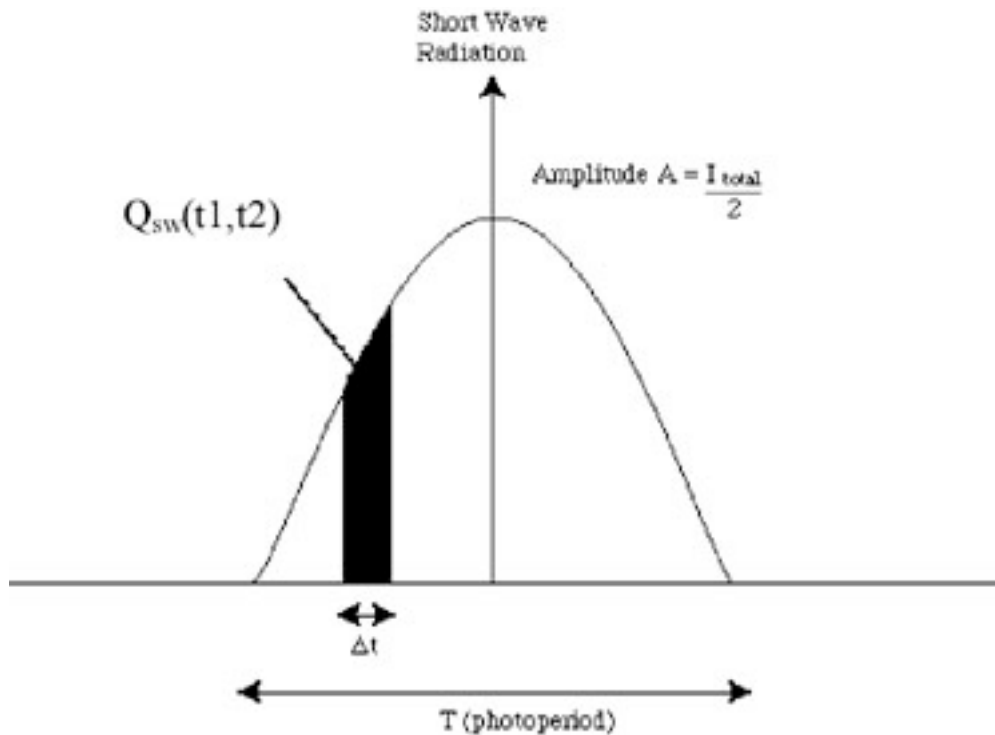


Figure 4.2 Short wave radiation distribution using daily average input data.

Thus, the shortwave energy per unit area entering layer j through its upper face is

$$\Delta Q_j = Q_j - Q_{j-1} \quad (4.16)$$

or

$$\Delta Q_j = Q_j \left(1 - e^{-\eta_{A_j} \Delta z_j}\right) \quad (4.17)$$

where η_{A_j} is the attenuation coefficient for the j^{th} layer, of thickness Δz_j , where

$$\Delta z_j = z_j - z_{j-1}; \quad (z_0 = 0, z_N = H) \quad (4.18)$$

where H is the depth of water.

For heating purposes, it is assumed that all of the ΔQ_j 's are converted to heat. Note that if $\Delta Q_j > 0$, heat is deposited, and if $\Delta Q_j < 0$, heat is removed from layer j .

Determine long wave energy flux

Longwave radiation is calculated by one of three methods, depending on the input data. Three input measures are allowed: incident long wave radiation, nett long wave radiation, and cloud cover.

1. Incident long wave radiation

Using incident long wave radiation requires accounting for albedo and long wave radiation emitted from the water surface. For daily data, the incident long wave radiation over a timestep is

$$Q_{lw(incident)} = \dot{Q}_{lw(incident)} \Delta t \quad (4.19)$$

where $\dot{Q}_{lw(incident)}$ is the average long wave radiative power density for the day. For sub-daily data, the incident longwave radiation over a timestep equals that in the input file. The long wave radiation penetrating the water surface is then

$$Q_{lw} = \left(1 - r_a^{(lw)}\right) Q_{lw(incident)} \quad (4.20)$$

where $r_a^{(lw)}$ is the albedo for long wave radiation, which is taken as a constant = 0.03 (Henderson-Sellers 1986).

Long wave radiation emitted from the water surface is given by (TVA 1972, eqn 3.5)

$$Q_{lw(emitted)} = \epsilon_w \sigma T_w^4 \quad (4.21)$$

where ϵ_w is the emissivity of the water surface ($=0.96$), σ is the Stefan-Boltzmann constant ($\sigma = 5.6697 \times 10^{-8} \text{ Wm}^{-2} \text{ K}^{-4}$), and T_w is the absolute temperature of the water surface (i.e. the temperature of the surface layer).

The nett longwave radiation energy density deposited into the surface layer for the period Δt is therefore

$$Q_{lw} = \left(1 - r_a^{(lw)}\right) Q_{lw(incident)} - \epsilon_w \sigma T_w^4 \quad (4.22)$$

2. Nett long wave radiation

Using net long wave radiation requires accounting for albedo at the water surface. For daily data, the incident long wave radiation over a timestep is

$$Q_{lw(nett)} = \dot{Q}_{lw(nett)} \Delta t \quad (4.23)$$

For sub-daily data, the incident long wave radiation over a timestep equals that in the input file. The long wave radiation energy density deposited into the surface layer for the period Δt is therefore

$$Q_{lw} = \left(1 - r_a^{(lw)}\right) Q_{lw(nett)} \quad (4.24)$$

3. Cloud cover

Long wave radiation can also be estimated from atmospheric conditions, using cloud cover fraction [0,1].

The nett long wave radiation energy density incident on the water surface can be estimated as

$$Q_{lw(rad)} = \left(1 - r_a^{(lw)}\right) Q_{lw(air)} \quad (4.25)$$

where (TVA 1972, eqn 3.14, Fischer et al.1979 eqn 6.21)

$$Q_{lw(air)} = (1 + 0.17C^2) \epsilon_a(T_a) \sigma T_a^4 \quad (4.26)$$

the subscript a referring to properties of the air. Swinbank (1963) showed that

$$\epsilon_a(T_a) = C_\epsilon T_a^2 \quad (4.27)$$

where $C_\epsilon = 9.37 \times 10^{-6} \text{ K}^{-2}$. As previously, the long wave emitted is given by equation 4.21

The nett long wave radiation is therefore

$$Q_{lw(rad)} = \left(1 - r_a^{(lw)}\right) (1 + 0.17C^2) \epsilon_a(T_a)\sigma T_a^4 - \epsilon_w\sigma T_w^4 \quad (4.28)$$

Determine the sensible heat flux

The sensible heat loss from the surface of the lake for the period Δt may be written as (Fischer et al. 1979 eqn 6.19)

$$Q_{sh} = C_S \rho_A C_P U_a (T_a - T_s) \Delta T \quad (4.29)$$

where C_S is the sensible heat transfer coefficient for wind speed at 10 m reference height above the water surface ($= 1.3 \times 10^{-3}$), ρ_A the density of air in kg m^{-3} , C_P the specific heat of air at constant pressure ($= 1003 \text{ J kg}^{-1} \text{ K}^{-1}$), U_a is the wind speed at the ‘standard’ reference height of 10 m in m s^{-1} , with temperatures either **both** in Celsius or **both** in Kelvin.

Determine the latent heat flux

The evaporative heat flux is given by (Fischer et al. 1979 eqn 6.20)

$$Q_{lh} = \min \left\{ 0, \frac{0.622}{P} C_L \rho_A L_E U_a [e_a - e_s(T_s)] \Delta T \right\} \quad (4.30)$$

where P is the atmospheric pressure in hectopascals, C_L is the latent heat transfer coefficient ($= 1.3 \times 10^{-3}$) for wind speed at the reference height of 10 m, ρ_A the density of air in kg m^{-3} , L_E the latent heat of evaporation of water ($= 2.453 \times 10^6 \text{ J kg}^{-1}$), U_a is the wind speed in m s^{-1} at the reference height of 10 m, e_a the vapour pressure of the air, and e_s the saturation vapour pressure at the water surface temperature T_S ; **both** vapour pressures are measured in hectopascals. The condition that $Q_{lh} \leq 0$, is so that no condensation effects are considered.

The saturated vapour pressure e_s is calculated via the *Magnus-Tetens* formula (TVA 1972, eqn 4.1):

$$e_s(T_s) = \exp \left[2.3026 \left(\frac{7.5T_s}{T_s + 237.3} + 0.7858 \right) \right] \quad (4.31)$$

where T_s is in degrees Celsius and e_s is in hectopascals.

Thus, the total non-penetrative energy density deposited in the surface layer during the period Δt is given by

$$Q_{non-pen} = Q_{lw} + Q_{sh} + Q_{lh} \quad (4.32)$$

4.1.3 Surface mass fluxes

Latent heat mass flux density

The change in mass in the surface layer (layer number N) due to latent heat flux is calculated as

$$\Delta M_N^{(lh)} = \frac{-Q_{lh} A_N}{L_v} \quad (4.33)$$

where A_N is the surface area of the surface layer and L_v is the latent heat of vaporisation for water.

Rainfall

It is assumed that the properties of the rain are the same as that of the surface layer. For daily data, the rainfall input for each timestep is

$$r_h = R_h \frac{\Delta t}{N_d} \quad (4.34)$$

where R_h is the daily total rainfall height. For sub-daily data, the rainfall over a timestep equals that in the input file. The change in surface layer mass is

$$\Delta M_n^{(rain)} = \rho_N A_N r_h \quad (4.35)$$

Total surface layer mass change

The total mass change of the surface layer for the period Δt is

$$\Delta M_n = \Delta M_n^{(lh)} + \Delta M_n^{(rain)} \quad (4.36)$$

In the current model, the change is due to evaporation and precipitation of pure water.

4.1.4 Surface momentum fluxes

Wind field

subsubsec:wind

The wind field in DYRESM drives both the surface layer shear and latent heat transfer. For daily meteorological data, the wind input into DYRESM is a daily average (over 24 hours) of the wind speed. For sub-daily meteorological data, the wind speed for the timestep is simply taken from the input *.met file.

Surface layer shear

A critical wind speed U_{crit} is used in the model, above which the wind is considered to drive motion in the surface layer. This value is set to 3 ms^{-1} in DYRESM.

Momentum exchange due to the wind begins only after the time at which the wind speed exceeds the critical value, that is when $U_a > U_{crit}$. Prior to this, the velocities in the layers U_i are set to zero for all layers. After the onset of the wind, the velocity in the surface layer U_N is calculated as (Fischer et al. 1979 eqn 6.54)

$$U_N = \frac{u_*^2}{\Delta Z_N} \Delta t \quad (4.37)$$

The shear velocity u_* is calculated from the wind speed by (Fischer et al. 1979 p.191)

$$U_* = \left(\frac{C_D \rho_a}{\rho_N} \right)^{1/2} U_a \quad (4.38)$$

where $C_D = 1.3 \times 10^{-3}$, ρ_N is the density of the surface layer, A_N the area of the surface layer, $\rho_a = 1.2 \text{ kg m}^{-3}$ (the density of air) and U_a is the wind velocity at a reference height of 10 metres.

For subsequent times, the velocity in the surface layer is

$$U_N(t + \Delta t) = U_N(t) + \frac{u_*^2}{\Delta Z_N} \Delta t \quad (4.39)$$

This continues until T_{sp} after the wind has increased above the critical value. T_{sp} is the shear period (defined below), and is the duration of time over which shear builds up in the surface layer. If the time T_{sp} is reached and the wind speed is still above the critical value, the layer speeds are set to zero, and the algorithm starts as if for a new wind event. If the wind speed drops below the critical value before the shear period is over, the layer speeds continue to build up as above until T_{sp} is reached. It is possible for the input wind speed U_a to be above the critical value. In this case, the wind will always put momentum into the surface layer.

Velocities in layers below the surface layer are changed through layer amalgamation, which has the effect of mixing momentum down through the water column.

Before applying the mixing algorithm, the characteristic layer speeds of the water column are set. These layer speeds depend on the wind stress and the temporal location within a shear period, if shear is switched on. The upper bound on the shear period is

$$T_{\max,sp} = \min(T_{limit}, T_{cor}) \quad (4.40)$$

where T_{cor} is the period based on the Coriolis effect,

$$T_{cor} = \frac{N_d}{\sin \theta} \quad (4.41)$$

where θ is the latitude, N_d the number of seconds in a day, and T_{limit} the maximum allowable limit for the shear period in the model, which is currently set to seven days.

The shear period used in the model is defined as

$$T_{sp} = \min \left(\frac{T_i}{4}, T_{\max, sp} \right) \quad (4.42)$$

where T_i is the internal seiche period. This is calculated as

$$T_i = \frac{A_N^{1/2}}{2c} \quad (4.43)$$

where $A_N^{1/2}$ is the basin length scale and c is the phase speed of the uninodal seiche (Fischer et al. 1979 eqn 6.11)

$$c = \sqrt{\frac{g}{\rho_{hypo}} (\rho_{hypo} - \rho_{epi}) \left(\frac{\Delta z_{epi} \Delta z_{hypo}}{\Delta z_{epi} + \Delta z_{hypo}} \right)} \quad (4.44)$$

where g is the gravitational constant, *epi* refers to the epilimnion, *hypo* to the hypolimnion, ρ is the volume-averaged layer density, and Δz is the layer thickness. The definition of the epilimnion and hypolimnion in the model are described in the following chapter.

4.1.5 Surface layers re-gridding

A technical issue may arise with modelling deep lakes. In order that the number of layers not become inordinately large (and, hence, increase the run-time) the user may be forced to set the maximum layer size to a large allowable thickness. The surface layer may then be too thick to allow accurate thermodynamic calculations to be made for the surface waters.

To ensure accurate surface layer thermodynamics with large maximum layer thicknesses DYRESM re-grids the top part of the water body to ensure that this part of the water column has a high enough resolution to enable ‘good’ thermodynamic calculations to be made. This surface layers re-gridding takes place before the distribution of energy into the water body occurs.

4.1.6 Atmospheric stability and surface exchange

One factor known to cause variability in the heat and momentum transfer described above is air column stability and water roughness (Imberger and Patterson 1990). This has the effect of altering the exchange coefficients C_S , C_L and C_D .

If the meteorological sensors are located within the internal boundary layer over the surface of the lake, and data is collected at sub-daily intervals, it is appropriate to consider the effect of air column stability on surface exchange. DYRESM uses the iterative procedure of Hicks (1975) to compute these values, as described in Imberger and Patterson (1990, p329). The user is referred to these references for more information.

Surface mixed layer algorithm

5.1 The Surface Mixing Model

5.1.1 Mechanisms

Three mechanisms are available to do the surface layer mixing in DYRESM:

1. convective overturn – where energy is released from the decrease in potential energy resulting from dense water falling to a lower level;
2. stirring – where energy from the wind stress is applied to the surface layer; and
3. shear – where kinetic energy is transferred from upper to the lower layers in the water column.

The method for modelling the surface mixed layer was described in detail by Yeates and Imberger (2003) and is given below.

5.1.2 Energetics

Turbulent Kinetic Energy (TKE) is introduced into the surface mixed layer (SML) through convective mixing (KE_{conv}), wind stirring (KE_{stir}), and shear mixing (KE_{shear}), using the parameterisations:

$$KE_{conv} = \eta_p \rho_N A_{N-1} w_*^3 \Delta t \quad (5.1)$$

$$KE_{stir} = \eta_s \rho_N A_{N-1} u_*^3 \Delta t \quad (5.2)$$

$$KE_{shear} = \frac{\eta_k}{2} \frac{M_N M_{N-1}}{M_N + M_{N-1}} (U_N U_{N-1})^2 \quad (5.3)$$

where η_p , η_s and η_k are efficiency coefficients, ρ_N the layer density, A_i the layer surface area, M_i the layer mass, U_i the layer speed and Δt the model time-step. Layers were indexed from $i = 1$ at the bottom to $i = N$ at the surface. The turbulent velocity scale due to convective overturn, is given by (Imberger and Patterson, 1981),

$$w_*^3 = \frac{g}{\rho_N \Delta t} \left\{ \sum_{i=K}^N \frac{\rho_i (h_i - h_{i-1}) (h_i + h_{i-1})}{2} - \frac{(h_N - h_{K-1})}{2} \sum_{i=K}^N \rho_i (h_i - h_{i-1}) \right\} \quad (5.4)$$

where h_i is the height of layer i and K is the final layer entrained into the SML during density stabilisation, which is performed at the beginning of each model time-step. u_* is the surface shear velocity due to wind, and is given by

$$u_* = \sqrt{\frac{C_D \rho_a}{\rho_w} U_H^2} \quad (5.5)$$

where C_D is the surface drag coefficient determined using the iterative procedure of Hicks (1975) and U_H is the wind speed at height H above the lake surface measured at each time-step. Fringing topographical features reduce surface wind stresses near the lake boundaries and therefore the concept of an effective area, A_E , was introduced to reduce A_N such that

$$A_E = A_N \tanh\left(\frac{A_N}{A_C}\right) \quad (5.6)$$

where A_C is the critical area and from Xenopoulos and Schindler (2001) is approximately 10^7 m^2 . Using A_E the transfer of momentum from surface stress becomes

$$U_N(t + \Delta t) = U(t) + \frac{u_*^2 A_E \Delta t}{V_N} \quad (5.7)$$

where V_N is the volume of the SML receiving the momentum. U_N was limited by allowing a maximum acceleration time of one-quarter the internal seiche period (Imberger and Patterson, 1981), after which U_N was re-set to zero. Momentum was conserved during layer deepening, and ultimately used to determine KE_{shear} and bottom shear.

5.1.3 Method

The mixing methods follows the procedure below

- During each time-step the SML routine calculates the potential energy required to mix layers N and $N - 1$, PE_{mix} , which is given by the expression

$$PE_{mix} = g [(M_N + M_{N-1}) \zeta_{N-1}^* - (M_N \zeta_N + M_{N-1} \zeta_{N-1})] \quad (5.8)$$

where z_i is the centre of mass of layer i and the asterisk superscript indicates the combined layer property after mixing.

- For an unstable density profile where $PE_{mix} < 0$, layers N and $N - 1$ are merged to form an updated SML with index $N = N - 1$ and this is continued until $PE_{mix} \leq 0$.
- The sum of available TKE, given by $KE_{avail} = KE_{conv} + KE_{stir}$, was then determined and if $KE_{avail} \leq PE_{mix}$ deepening of the SML continues and with each layer entrainment KE_{avail} was reduced by amount PE_{mix} .
- When $KE_{avail} < PE_{mix}$ for the first time the momentum of the surface layer is updated (i.e. U_N) and KE_{avail} is augmented with KE_{shear} .

- The condition $KE_{avail} \leq PE_{mix}$ is then re-assessed and if met deepening continues with KE_{avail} augmented by KE_{shear} at each layer interface.
- When $KE_{avail} < PE_{mix}$ for the second time, mixing ceased and any remaining KE_{avail} was carried forward for use in the next time step.
- If the routine encounters the bottom before the condition $KE_{avail} < PE_{mix}$ was achieved the remaining energy is lost.

5.1.4 Epilimnion and hypolimnion information

After mixing has taken place, epilimnion and hypolimnion heights and densities are stored for possible use in the next time step, for use in the calculation of the shear period. The epilimnion height and density values are those of the newly mixed and deepened surface layer. The hypolimnion height and density values are taken to be those of the layer immediately below the newly mixed surface layer.

5.1.5 Bottom stresses

If water quality is to be simulated using CAEDYM, bottom stress magnitudes need to be calculated, and then passed to the CAEDYM algorithms for resuspension. This requires that epilimnion and hypolimnion water speeds be determined, U_E and U_H , respectively. From the mixing just completed, a value for U_E is available and is equal to U_N , the velocity of the surface layer.

The velocity in the hypolimnion is calculated by

$$U_H = \begin{cases} \frac{U_E h_E}{h_H}; & h_E < h_H \\ U_E; & h_E \geq h_H \end{cases} \quad (5.9)$$

where h_H and h_E are the thicknesses of the hypolimnion and epilimnion, respectively. The first condition is obtained from conservation of volume in a rectangular basin, with the second condition taken so as to avoid high unrealistic values for U_H when the mixed layer is the dominant fraction of the water column.

The magnitudes of the bottom stress for the epilimnion and hypolimnion can now be directly calculated

$$\tau_E = C_{D,bottom} \rho_E U_E^2 \quad (5.10)$$

$$\tau_H = C_{D,bottom} \rho_H U_H^2 \quad (5.11)$$

where $C_{D,bottom}$ is the bottom drag coefficient.

Inflow Dynamics

6.1 Inflow Dynamics

Inflows into DYRESM may be either surface or subsurface flows. A surface flow will be due to a river or stream, whereas a subsurface flow could be due to either groundwater or a pipe inflow. Subsurface inflows can be either buoyant or dense compared to the ambient fluid at the level of inflow, and so different algorithms are used for these two cases. The case of a dense, subsurface inflow uses the same algorithm as the surface inflow model.

6.1.1 Surface Inflow

Introduction

The surface inflow process may be divided into three stages. As a stream enters the lake it will push the stagnant water ahead of itself until buoyancy forces, due to the density differences which may be present, have become sufficient to arrest the flow. At this point the flow either floats over the reservoir surface if the inflow is lighter than the lake water or it plunges beneath the reservoir water if it is heavier. If the entrance point to the reservoir is a well defined drowned river valley, then the side of the valley will confine the flow and a plunge line will be visible across the reservoir at which point the river water submerges uniformly and travels down the channel in a one dimensional fashion.

The possible inflow scenarios are shown schematically in Figure 6.1. These different inflow patterns must now be considered in terms of a modelling approach.

Initialisation

For all inflows, the values of the drag coefficient of the river bed C_D , the slope angle of the inflow ϕ , the stream half angle α and the entrainment coefficient constant E are read in. The entrainment coefficient is given by (Dallimore et al., 2001)

$$E = \frac{C_k C_D^{3/2} + C_S}{R_{in} + 10 (C_k C_D^{3/2} + C_S)} \quad (6.1)$$

where C_D is the drag coefficient, C_K and C_S are shape parameters and are fixed at 2.2 and 1×10^{-4} , respectively, R_{in} is the bulk Richardson number of the inflow, and is given by (Fischer et al., 1979; Eqn. 6.105)

$$R_{in} = \frac{4E + \frac{5C_D}{\sin \alpha}}{5 \tan \phi - \frac{8E}{3}} \quad (6.2)$$

Equations (5.1) and (5.2) are solved once simultaneously for each inflow at the start of the simulation to give the parameters E and R_{in} for the remainder of the simulation.

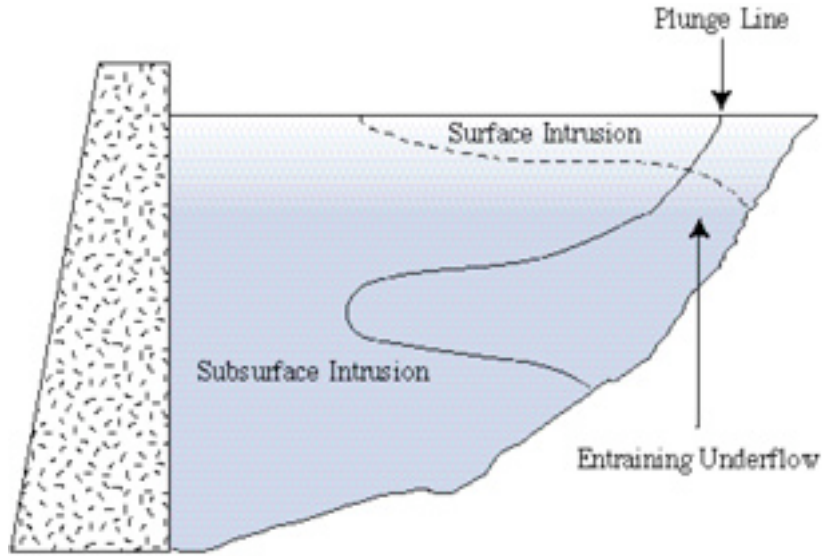


Figure 6.1 Possible river inflow patterns.

Downflow

Once the inflowing river has negotiated the plunge line it will continue to flow down the river channel, entraining reservoir water as it moves towards the dam wall. The downflow time may be several days and is further complicated by the entrainment of lake water into the inflowing volume during this downflow process.

At the start of the plunge into the lake, the initial thickness of the inflow, h_o , is given by (based on Imberger and Patterson, 1982; Eqn. 58)

$$h_o = \left(\frac{2\dot{Q}_{alq}^2 R_{in}}{g' \tan^2 \alpha} \right)^{1/5} \quad (6.3)$$

where

$$g' = \frac{\rho_{inflow} - \rho_{surface}}{\rho_{inflow}} g \quad (6.4)$$

is the reduced gravity, rate of inflow is the volume flow rate of inflow for the day ($\text{m}^3 \text{s}^{-1}$) and \dot{Q}_{alq} denotes the inflow aliquot for the day.

As the aliquot flows downflows, it entrains water from each layer it passes through, thus changing the aliquot's properties. The amount of water entrained from a layer into the downflowing aliquot is determined by the aliquot's frontal thickness and current volume. The increase ΔQ_{alq} in the underflow aliquot volume Q_{alq} is given by the conservation of volume (Imberger and Patterson, 1981; Eqn. 57)

$$\Delta Q_{alq} = Q_{alq} \left[\left(\frac{h}{h_{prev}} \right)^{5/3} - 1 \right] \quad (6.5)$$

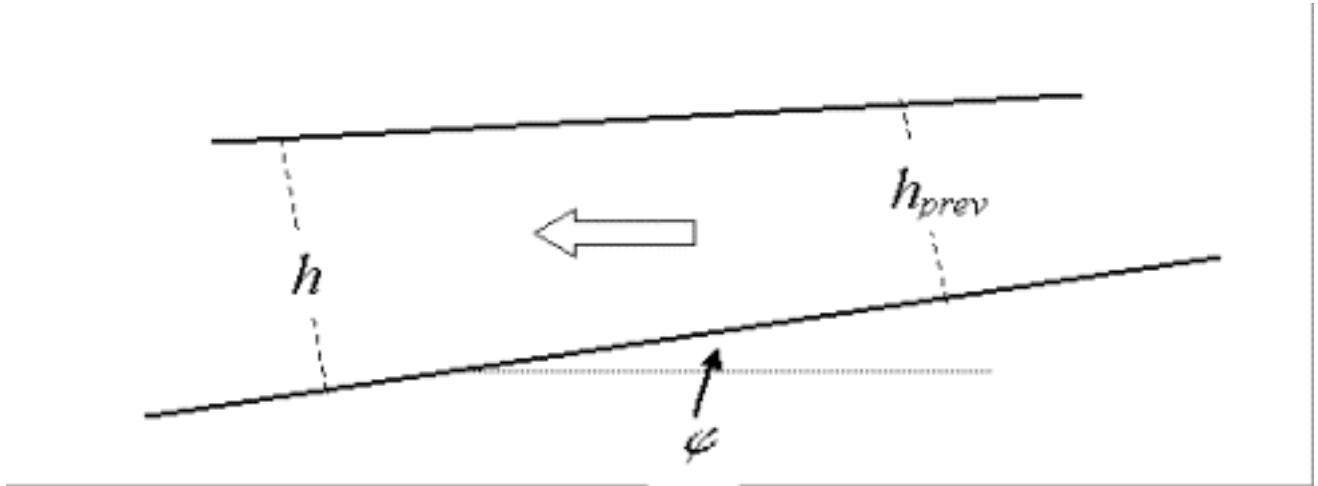


Figure 6.2 Schematic diagram of downflow aliquot

where h_{prev} is the frontal thickness for the previous layer, and h the frontal thickness for the current layer after entrainment. The height after entrainment h is given by (assuming a triangular cross section where $a = h \tan \alpha$) (Fischer et al., 1979; Eqn 6.112)

$$h = 1.2E_s + h_o \quad (6.6)$$

where s is the slope distance from the surface.

The process of entrainment is repeated for each layer until the aliquot reaches a position in the water body of neutral buoyancy (or the lake bottom), at which point a layer is created in the water body and filled with the aliquot.

Insertion

The entrainment given by equation (6.5) leads to a decrease in the density of the plunging inflow until at some level, the inflow and reservoir densities balance and the inflow penetrates the reservoir .

Solution Method

Introduction

The entrance of the river inflow into the reservoir is modeled by the insertion of a volume into a number of existing layers at the appropriate height. If the layer volumes become excessive, new layers are formed. The increased volume of these layers causes those above to move upwards, decreasing their thickness in accordance with the given volume-depth relationship, to accommodate the volume increase.

Step 1: Initialisation

- The inflow properties of volume Q , temperature T , salinity S , and density ρ are initialised to the corresponding river values. The inflow density ρ is then computed using the UNESCO equation of state as defined in section 3.1.4. The inflow density is then compared with the density of the surface layer.
- If $\rho_{inflow} \leq \rho_{surface}$ then the total volume is added to the top layer, a new surface level and properties are computed, and the control is returned to the main program.
- If $\rho_{inflow} > \rho_{surface}$ then underflow occurs and entrainment calculations are necessary.

Step 2: Entrainment Calculations

For each inflow the entrainment ΔQ is calculated. The entrainment from the layers adjacent to the underflow is computed from Eq. (6.5) and this quantity of water is added to the inflow volume Q . The properties are adjusted and the density compared with the next lowest layer. If the inflow density is smaller, a new layer is created and filled with the inflow aliquot. If not, the process is repeated until the particular inflow has reached its neutrally buoyant level or the bottom is reached. Each inflow is routed to its neutrally buoyant level instantaneously.

Step 3: Insertion If an inflow has reached its level of neutral buoyancy, it is inserted instantaneously as a new layer at that height. The layer structure is then checked for layer amalgamation based on layer limits set for the simulation.

6.1.2 Subsurface inflow

Introduction

The subsurface inflow process is split depending on whether the inflow is lighter or denser than the ambient water at the depth of the inflow. For a dense inflow, the model outlined above for surface inflows is followed. For a buoyant subsurface inflow, the flow is modelled as a simple, single-phase plume with circular cross-section. When the upwards buoyancy flux due to the density anomaly becomes zero due to the entrained ambient water, the plume inserts.

Initialisation

The plume is initialised by first computing the upwards buoyancy flux due to the density difference between the inflowing aliquot and the ambient fluid at the height of the inflow, as (Fischer et al. 1979, eqn 9.7)

$$B_i = g \left(\frac{\rho_i - \rho_{inf}}{\rho_i} \right) Q_{inf} \quad (6.7)$$

where Q_{inf} is the inflow flow rate (m^3s^{-1}), ρ_{inf} is the density of the inflowing water and ρ_i is the ambient density of layer i , at the height of the inflow.

The flow rate of the plume (inflow plus entrained water) is computed as (Fischer et al., 1979; Eqns. 9.28, 9.30, 9.107)

$$Q_P = \alpha \frac{6\pi}{5} b_1 L_R B^{1/3} (z_i - z_{inf})^{5/3} + Q_{inf} \quad (6.8)$$

where B is the buoyancy flux (m^4s^{-3}), z_i is the layer height, z_{inf} is the height of the inflow, b_1 is a constant (= 4.7, Fischer et al., 1979; p329), L_R is the plume aspect ratio (plume radius to plume length, assumed to be a constant of 0.1), and a is an entrainment coefficient. This value has been found experimentally to be 0.083.

Subsequent entrainment

The flow rate of the entrained volume in layer i is calculated as

$$Q_P = \alpha \frac{6\pi}{5} b_1 L_R B^{1/3} (z_i - z_{inf})^{5/3} + Q_{P_{i-1}} \quad (6.9)$$

where the buoyancy flux now accounts for the entrained water

$$B_i = g \left(\frac{\rho_i - \rho_P}{\rho_i} \right) Q_P \quad (6.10)$$

Detrainment

When the buoyancy flux B becomes zero or negative, or the plume reaches the water surface, the entrained water is entrained instantaneously into the current layer. For the case of the plume reaching the surface, a new layer is created on the surface of the reservoir containing only the plume water.

Outflow Dynamics

7.1 Outflow Dynamics

The term ‘outflow’ refers to the combination of withdrawals and overflow.

7.1.1 Withdrawal

subsec:wdwal

For each outlet the following algorithm is executed.

1. The level of the outlet is determined and the required quantity Q is extracted from the layer adjacent to this outlet.
2. If Q exceeds the volume of this layer then water is taken from successive layers above the outlet until the required volume Q is removed from the water column.
3. The layer structure is re-determined after each layer has been altered.

7.1.2 Overflow

All water above the crest height is removed from the top of the water body. If there is initially more than one layer above the crest height, then all layers above crest height are removed and a proportion of the remaining layer is removed such that the surface height of the resulting water body is equal to the crest height.

7.1.3 Data Output

The water properties (*e.g.* temperature, DO, FE) which have been selected by the user to be output during the simulation are output not only for the water column but also for each withdrawal and overflow ‘device’ (*i.e.*, an aliquot of water for each time step and for each device). For each outflow aliquot the volume is written to the program output as well as the selected water properties. If water from more than one layer is required for an aliquot then the resulting aliquot properties are the averaged values for each property.

Deep Mixing

8.1 Deep Mixing

8.1.1 Introduction

The mixed layer algorithm allows the depth of the surface mixed layer (SML) to be calculated. Below the SML the waters the density gradients range from strong in the metalimnion to weak in the hypolimnion and have a stabilizing effect on the water column that restricts vertical mixing to small levels.

The mixing mechanisms that occur deep in lakes can be categorised into three broad groups (Imberger and Patterson 1981). Firstly, internal wave interactions leads, under the right conditions, to a growth of one wavelength at the expense of others until breaking occurs. Secondly, the local shear may be raised, by combining of long and short internal waves, to such a level that Kelvin-Helmholtz billowing can take place. Thirdly, gravitational overturning can be induced by absorption of wave energy at critical layers.

A model that would attempt to describe these processes would be very complex and difficult to verify due to the nature of internal wave dynamics and our limited understanding of the processes. To avoid these complexities DYRESM takes a parameterisation approach to modelling the deep mixing processes in lakes.

In DYRESM deep mixing is separated into two parts: 1) internal mixing and 2) benthic boundary layer (BBL) mixing. Both these mechanisms are invoked in DYRESM only once per day (at midnight at the start of each day).

1. ‘Internal mixing’ encompasses the effects of two mixing mechanisms together: molecular diffusion and shear mixing.

For each layer a calculated proportion of the volume is removed and transferred into the layer immediately above it. Similarly, the same volume is mixed from the upper layer into the current layer of interest. This process continues from bottom to top through the water column.

2. BBL mixing is parameterised in a similar fashion to wind stirring in the surface layer. The kinetic energy available to mix the water adjacent to the boundary is determined from shear velocities at the bottom sediment. Fluid entrained into the benthic boundary layer is treated separately from ‘internal’ fluid producing a pseudo two-dimensional model with an explicit boundary layer (see Yeates and Imberger 2003).

8.1.2 Solution Method

BBL and Internal mixing

BBL and internal mixing are done once per day and at the start of each day. These two mechanisms are not invoked whenever the water column is fully mixed at the start of the day. The details of this BBL and internal mixing procedure are given in Yeates and Imberger (2003) and a summary is provided below.

DYRESM uses the Lake Number (L_N) (Imberger and Patterson, 1990; Eqn. 2.7) and buoyancy frequencies (N^2) of the water column to determine the amount of water to mix from one layer to another. The Lake Number is calculated once per day by using day-averaged values of its parameters; N^2 is calculated at all the layer boundaries of the water column.

The volume of water transferred from layer i to $i + 1$ and, simultaneously, from layer $i + 1$ to i is given by

$$F_i^T = \frac{200N_i^2 A_i K_M \Delta t}{L_N N_{MAX}^2 \left(\frac{\delta_i + \delta_{i+1}}{2} \right)} \quad (8.1)$$

where Δt is the model time step, N_i is the buoyancy frequency determined between layers i and $i + 1$, K_M is the molecular diffusivity of heat and δ_i and δ_{i+1} are layer thicknesses. The purpose of normalising with respect to the maximum buoyancy frequency (N_{MAX}^2) is to ensure that internal mixing in the water column is maximised at the seasonal thermocline. The coefficient of 200 has been determined by fitting a relationship between field estimates of eddy diffusivity and Lake Number in a range of lakes (Yeates and Imberger 2003).

The total volume flux is then partitioned into a BBL exchange, F_i^B , and an internal exchange, F_i^I , using the expression

$$F_i^I = \begin{cases} \frac{F_i^T \tanh(B_N)(L_N - 1)}{L_N}, & L_N > 1 \\ 0, & L_N \leq 1 \end{cases} \quad (8.2)$$

with $F_i^B = F_i^T - F_i^I$, always.

The layer structure in previous versions of DYRESM consisted of a Lagrangian vertical grid with user-specified maximum and minimum allowable layer thicknesses. While this framework remains essentially unchanged, a pseudo two-dimensional BBL structure is now implemented so that each layer (i) consists of a BBL cell (BC_i) and an internal cell (IC_i). At the start of each day, BBL heights are updated (see below) and the BC_i and IC_i volumes are derived from the bathymetry. If the BBL height increases, water is entrained from the IC_i into the BC_i , and if BBL height decreases, the entrainment is reversed. When a layer is entrained into the surface mixed layer by the surface mixing model the BBL thickness of that layer is re-set to zero and the volume in BC_N is transferred into IC_N (the subscript N is the layer counter of the surface layer). However, during splitting or merging of layers in response to grid changes the boundary cells and internal cells remain independent, communicating only with their adjacent counterparts. Inflow plumes are initially inserted with no initial BBL volume and outflow and entrainment losses are partitioned between internal and BBL cells.

Volume fluxes F_i^B and F_i^I are transferred from cells BC_i to BC_{i+1} and IC_i to IC_{i+1} respectively, starting from the bottom layer and ending at layer N at the surface. Simultaneous fluxes of equal volume are returned in the opposite direction to mimic the upward and downward fluxes in turbulent mixing events and to conserve cell volumes so that layer structures do not need to be altered after each exchange. If the volume of BC_i is less

than F_i^B the remainder is directed through the neighbouring internal cells and vice versa, to ensure that the total volume of the exchange between layers is completed. In the surface mixed layer (layer index N), there is no BBL and the flux from BC_{N-1} is directed into IC_N .

BBL height

The height the BBL is updated once each day by evaluating the kinetic energy produced at the boundary due to bottom shear stress and assessing the height of water that can be entrained into the BBL. The height of the BBL (h_b) is updated at the end of each day using the parameterization (following Lemckert et al 2004)

$$h_b(t + \Delta t)^3 = h_b(t)^3 + \frac{6C_k^* u_b^{*3}}{N_i^2} \Delta t \quad (8.3)$$

where $C_k^* = 0.23$ is the efficiency of TKE generation at the boundary and u_b^* is the mean daily bottom shear velocity. Bottom shear velocity is determined by applying a user-defined bottom drag coefficient and estimating the hypolimnion velocity from the surface velocity by invoking the continuity of momentum for a rectangular basin. BBL heights are updated for each layer and the volume of BC_i adjusted according to height and bathymetric area. A constant eddy diffusivity is assumed at the top of the BBL and acts to detrain water from the BBL and balance the growth term (Gloor et al. 2000).

Artificial Destratification

9.1 Artificial Destratification

There are currently two types of destratification systems that DYRESM can model – bubble plume diffusers and surface mechanical mixers (impellers) with draft tubes:

- Bubble plume diffusers consist of a perforated pipe beneath the surface of the water, through which compressed air is pumped. As the air rises through the water column, it entrains fluid and mixes the water column.
- Surface mechanical mixers with draft tubes consist of a large impeller mounted at the surface pointing vertically downwards. Surrounding the impeller is a non-permeable curtain (a draft tube), through which water is impelled until escaping at the end of the draft tube. Once reaching the end of the draft tube, the water rises, entraining ambient water and mixing the water column.

DYRESM allows night-time, day-time or 24-hour operation of the destratification system. The destratifier system may be composed of bubbler and impeller devices.

9.1.1 Bubble Plume Diffusers

Introduction

The bubble plume destratification in the DYRESM model uses the simple buoyant plume equations, and assumes the plumes are circular and non-interacting. Air is pumped to depth, and released into the water column via a diffuser. The bubbles rise, entraining ambient water. When the upwards buoyancy flux due to the air bubbles is equal to the downwards force (due to gravity) of the entrained ambient water, the bubble plume sheds the entrained water. This water is immediately routed to its neutrally buoyant level, without entrainment.

The bubble plume then begins to entrain ambient water again, until it reaches the surface where any entrained water is shed, and again routed to its neutrally buoyant level.

The bubbler is run on the sub-daily time step of the model.

Initialisation

The bubbler is initialised by first computing the upwards buoyancy flux due to the air, as (Fischer et al. 1979, eqn 9.7)

$$B_{air} = gQ_{diff} \quad (9.1)$$

Note that the air flow rate MUST be that at the level of the diffuser, not the free-air flow rate of the compressor. The correction can be made by assuming that air is in ideal gas and is adiabatically compressed according to (Wallace and Hobbs 1977, p89)

$$Q_{diff} = Q_{air} \left(\frac{P_{air}}{P_{diff}} \right)^{0.71} \quad (9.2)$$

where Q_{air} is the free air flow rate of the compressor, P_{air} is the air pressure (usually taken as 101.3 kPa), P_{diff} the pressure at the level of the diffuser due to both the atmosphere and the depth of water, and Q_{diff} the diffuser air flow rate.

Once the value of Q_{diff} is passed into the model, it is divided by the number of ports (or clusters) to determine the flow rate per port. All subsequent calculations are done on a per port basis, then multiplied by the total number of ports to get the total effect of the destratification system.

The flow rate of entrained water is computed as (Fischer et al. 1979, eqns 9.28, 9.30, 9.107)

$$Q_P = \alpha \frac{6\pi}{5} b_1 L_R B^{1/3} z^{5/3} \quad (9.3)$$

where B is the buoyancy flux [m^4/s^3], z is the bottom layer thickness [m], b_1 is a constant ($= 4.7$ - Fischer et al. 1979, p329), L_R is the plume aspect ratio (plume radius to plume length, assumed to be a constant of 0.1), and α is an entrainment coefficient.

Subsequent entrainment

The first step is to compute the flow rate of air, which will increase due to decreasing pressure leading to adiabatic expansion of the bubbles. The new flow rate (due to adiabatic expansion) in layer i can be calculated as

$$Q_i = Q_{i-1} \left(\frac{P_{i-1}}{P_i} \right)^{0.71} \quad (9.4)$$

where layer $(i - 1)$ refers to the layer below, and pressure P has units of Pascals.

The combined buoyancy flux of the air bubbles and entrained water is calculated as

$$B_i = gQ_i - g \left(\frac{\rho_i - \rho_P}{\rho_i} \right) Q_P \quad (9.5)$$

where ρ_i is the density of the current layer, and Q_P is the flow rate of the entrained volume. The second term is the reduction in buoyancy flux due to the entrained water the plume is dragging with it.

The flow rate of the entrained volume in layer i is calculated as

$$Q_P = \alpha \frac{6\pi}{5} b_1 L_R B_i^{1/3} \left(z_i^{5/3} - z_{i-1}^{5/3} \right) + Q_{P_{i-1}} \quad (9.6)$$

Detrainment

When the combined buoyancy flux (equation 9.5) becomes negative, the entrained water detrains from the air plume. It is then routed to its neutrally buoyant level instantaneously.

The plume characteristics are then reset, and the air continues to rise and begins entraining water again.

9.1.2 Surface mechanical mixers with draft tubes

Introduction

It is assumed the water acts as a buoyant plume upon exiting the draft tube. The current implementation will NOT model jet behaviour, and so if the model is configured such that a jet flow is likely to result, incorrect results will be produced. The plume is modelled as a line plume, wrapped around the circumference of the draft tube, where the draft tube is assumed circular.

Initialisation

The plume is initialised by first computing the upwards buoyancy flux due to the difference in density between the water in the draft tube (assumed to have the same properties as the surface layer water) and the water at the base of the draft tube (Fischer et al 1979, eqn 9.7)

$$B = g \frac{\rho_{base} - \rho_{plume}}{\rho_{base}} \frac{Q_P}{\pi D} \quad (9.7)$$

where ρ_P is the plume density (initially assumed to be the surface density), ρ_{base} is the density of ambient water at the base of the draft tube, Q_P is the daily average impeller flow rate (m^3s^{-1}), and D is the draft tube diameter (m). The units of B are (m^3s^{-3}), which describes the buoyancy flux per unit length for a line plume (Kotsovinos and List 1975 eqn 2.8, Fischer et al. 1979 Table 9.3).

The new flow rate due to the entrained water is computed as (Fischer et al. 1979 Table 9.3, also p366)

$$Q_{P_i} = 3.32\alpha (\pi D) B^{1/3} \Delta z_j + Q_P \quad (9.8)$$

where Δz_j is the starting layer thickness (the layer thickness at the base of the draft tube), and α is an entrainment coefficient, found experimentally to be 0.1024 (Fischer et al. 1979, Table 9.3, from Kotsovinos). This number has been halved for this application, as ambient water is only being entrained along one side of the plume due to the vertical barrier of the draft tube.

Subsequent entrainment

After each layer, the new plume density ρ_P is calculated. The buoyancy flux B_j in layer j is computed as

$$B_j = g \frac{\rho_j - \rho_{P_{j-1}}}{\rho_j} \frac{Q_{P_{j-1}}}{\pi D} \quad (9.9)$$

where $(j - 1)$ indexes the layer below the current layer. The new plume volume is calculated as

$$Q_{P_i} = 3.32\alpha (\pi D) B_j^{1/3} \Delta z_j + Q_{P_{j-1}} \quad (9.10)$$

Detrainment

When the plume reaches neutral buoyancy (that is when the buoyancy flux becomes zero), the plume is instantaneously inserted. As the plume is single phase, there is no reinitialisation after detrainment, as occurs with bubble plumes.

Bibliography

1. Dallimore, C.J., J. Imberger and T. Ishikawa. 2001. Entrainment and turbulence in a saline underflow in Lake Ogawara. *ASCE Journal of Hydraulic Engineering*, 127(11):937-948.
2. Fischer, H. B., List, E. G., Koh, R. C. Y., Imberger, J., and Brooks, N. H. 1979. *Mixing in Inland and Coastal Waters*. Academic Press.
3. Gates, D.M. 1966. Spectral distribution of solar radiation on the earth's surface. *Science*, 151:523-529.
4. Gloor, M., A. Wuest and B.M. Imboden. 2000. Dynamics of Mixed Bottom Boundary Layers and its Implication for Diapycnal Transport in a Stratified, Natural Water Basin. *J. Geophys. Res.*, 105(C4):8629-8646.
5. Henderson-Sellers, B. 1986. Calculating the surface energy balance for lake and reservoir modelling: a review. *Reviews of Geophysics*, 24(3):625-649.
6. Hicks, B.B. 1975. A procedure for the formulation of bulk transfer coefficients over water. *Boundary Layer Meteorology*, 8:315-324.
7. Imberger, J. 1985. The diurnal mixed layer. *Limnol. Oceanogr.*, 30:737-770.
8. Imberger, J. and P.F. Hamblin. 1982. Dynamics of lakes, reservoirs and cooling ponds. *Ann. Rev. Fluid Mech.*, 14:153-187.
9. Imberger, J. and Patterson, J. C. 1981. A dynamic reservoir simulation model - DYRESM:5. In "Transport Models for Inland and Coastal Waters", pp310-361, H.B. Fischer (ed). Academic Press.
10. Imberger, J. and Patterson, J. C. 1990. Physical limnology. *Advances in Applied Mechanics*, 27:303-455.
11. Jellison, R., and J.M. Melack. 1993. Meromixis in hypersaline Mono Lake, California. Stratification and vertical mixing during the onset, persistence and breakdown of meromixis. *Limnol. Oceanogr.* 38:1008-1019.
12. Kotsovinos, N.E. and E.J. List. 1975. Plane turbulent buoyant jets. Part I. Integral properties. *J. Fluid Mech.*, 81:25-44.
13. Lemckert, C.J., J.P. Antenucci, A. Saggio and J. Imberger. 2004. Physical properties of turbulent benthic boundary layers generated by internal waves. *ASCE Journal of Hydraulic Engineering*, 130(1):58-69.
14. Patterson, J. C., Hamblin, P. F., and Imberger, J. 1984. Classification and dynamics simulation of the vertical density structure of lakes. *Limnology and Oceanography*, , 29:845-861.

15. Swinbank, W. C. 1963. Longwave radiation from clear skies. *Quarterly Journal of the Royal Meteorological Society*, 89:339-348.
16. Tennessee Valley Authority. 1972. Heat and mass transfer between a water surface and the atmosphere. Water Resources Research Laboratory Report 14, Report No. 0-6803.
17. Unesco. 1981. *Technical papers in Marine Science*. No. 36.
18. Wallace, J.M. and P.V. Hobbs. 1977. Atmospheric Science: an introductory survey. Academic Press
19. Xenopoulos, M. A., and D. W. Schindler. 2001. The environmental control of near-surface thermoclines in boreal lakes. *Ecosystems*, 4:699-707.
20. Yeates, P.S. and J. Imberger. 2003. Pseudo two-dimensional simulations of internal and boundary fluxes in stratified lakes and reservoirs. *Intl. J. River Basin Management*, 1(4):279-319.